Microemulsions with Surfactant TX100, Cyclohexane, and an Ionic Liquid Investigated by Conductance, DLS, FTIR Measurements, and Study of Solvent and Rotational Relaxation within th...

ARTICLE *in* THE JOURNAL OF PHYSICAL CHEMISTRY B · JUNE 2010

Impact Factor: 3.3 · DOI: 10.1021/jp1017086 · Source: PubMed

6 AUTHORS, INCLUDING:

Chiranjib Ghatak
University of Kansas
38 PUBLICATIONS **570** CITATIONS
SEE PROFILE

Vishal Govind Rao
Bowling Green State University
49 PUBLICATIONS **533** CITATIONS
SEE PROFILE

Nilmoni Sarkar
IIT Kharagpur
159 PUBLICATIONS **3,691** CITATIONS
SEE PROFILE

Microemulsions with Surfactant TX100, Cyclohexane, and an Ionic Liquid Investigated by Conductance, DLS, FTIR Measurements, and Study of Solvent and Rotational Relaxation within this Microemulsion

Rajib Pramanik, Souravi Sarkar, Chiranjib Ghatak, Vishal Govind Rao, Palash Setua, and Nilmoni Sarkar*

Department of Chemistry Indian Institute of Technology, Kharagpur 721302, WB, India

Received: February 25, 2010; Revised Manuscript Received: April 24, 2010

Room-temperature ionic liquids (RTILs), *N*,*N*,*N*-trimethyl-*N*-propyl ammonium bis(trifluoromethanesulfonyl) imide ($[N_{3111}][Tf_2N]$), were substituted for polar water and formed nonaqueous microemulsions with cyclohexane by the aid of nonionic surfactant TX-100. The phase behavior of the ternary system was investigated, and microregions of $[N_{3111}][Tf_2N]$-in-cyclohexane (IL/O), bicontinuous, and cyclohexane-in-$[N_{3111}][Tf_2N]$ (O/IL) were identified by traditional electrical conductivity measurements. Dynamic light scattering (DLS) revealed the formation of the IL microemulsions. The FTIR study of O−H stretching band of TX100 also supports this finding. The dynamics of solvent and rotational relaxation have been investigated in $[N_{3111}][Tf_2N]$/TX100/cyclohexane microemulsions using steady-state and time-resolved fluorescence spectroscopy as a tool and coumarin 480 (C-480) as a fluorescence probe. The size of the microemulsions increases with gradual addition of $[N_{3111}][Tf_2N]$, which revealed from DLS measurement. This leads to the faster collective motions of cation and anions of $[N_{3111}][Tf_2N]$, which contributes to faster solvent relaxation in microemulsions.

1. Introduction

Room-temperature ionic liquids (RTILs) are an interesting class of tunable, designer solvents with essentially zero volatility. RTILs are composed of sterically mismatched ions[1,2] that hinder crystal formation. Because the properties of the RTILs are very much dependent on the constituent ions, various RTILs can be designed using appropriate combination of the cationic and anionic constituents for some desired properties. The most popular cationic components of the RTILs are imidazolium, pyridinium, and ammonium derivatives and anions such as $[PF_6]^-$, $[BF_4]^-$, $[CF_3SO_3]^-$, and $[(CF_3SO_2)_2\ N]^-$ (abbreviated as $[Tf_2N]^-$). We have used *N*,*N*,*N*-trimethyl-*N*-propyl ammonium bis(trifluoromethanesulfonyl) imide $[N_{3111}][Tf_2N]$ as RTILs in our work. Solvation properties of RTILs are comparable to those of highly polar solvents, and they have already found use in synthesis and catalytic reactions.[2] Despite these features, solubility limitations for apolar solutes remain, which could be overcome by incorporation of hydrocarbon domains provided by normal micelles or formation of ionic liquid-in-oil (IL-O) microemulsions. The properties of microemulsions with nanometer-sized water clusters[3−8] or strong polar organic solvent cores[9−12] have been studied extensively. As neoteric solvents, RTILs are receiving much attention in diverse fields because of their special physical and chemical properties,[13,14] such as strong solvating power for both organic and inorganic compounds, very low volatility, and high thermal stability. They are also regarded as "green" solvents for chemical reactions,[15,16] extraction and fractionations,[17] and material preparation.[13,14] The significance is that nanostructured surfactant assemblies would provide hydrophobic or hydrophilic nanodomains, thereby expanding potential uses of RTILs as reaction and separation or extraction media.

Microemulsions are optically transparent, isotropic, thermodynamically stable solution mixtures of at least three components, namely, two immiscible solvents and a surfactant. The surfactant (sometimes in combination with a cosurfactant) separates the two solvents by forming a monolayer at the liquid−liquid interface. Kahlweit et al. performed numerous systematic experiments aimed to generalize the behavior of microemulsions.[18−21] In a recent review, the general pattern of the phase behavior, properties, and microstructure of microemulsions are summarized.[22] However, because of environmental hazards, researchers are trying to find alternatives for organic solvents. Recently, RTILs have been successfully used to replace either water or organic solvents in microemulsions. Han and coworkers first discovered that 1-butyl-3-methylimidazolium tetrafluoroborate ($bmimBF_4$) assembled in polar nanosized droplets when dispersed in cyclohexane as solvent, and the RTIL microemulsions showed a regular swelling behavior similar to water-in-oil (W/O) microemulsions; that is, the volume of the dispersed nanodroplets is directly proportional to the amount of added RTIL.[23] Recently, several groups prepared and characterized RTILs containing micelles and microemulsions.[24−28]

Several photophysical, theoretical, and ultrafast spectroscopic studies have been carried out in RTILs and RTIL-containing microheterogeneous systems.[29−39] There were several studies on solvation dynamics in neat RTILs[39−42] after the first report of Samanta and coworkers.[43] Solvation dynamics in an RTIL occurs in a slow nanosecond time scale along with a subpicosecond component.[43−45] To understand the solvation process in RTILs, several groups carried out computer simulations on the structure and dynamics in a RTIL.[46] These simulations suggest that solvation dynamics in an RTIL involves collective motion of the cation and the anion.[46] The solvation dynamics has also

* Corresponding author. E-mail: nilmoni@chem.iitkgp.ernet.in. Fax: 91-3222-255303.

10.1021/jp1017086
Published on Web 05/14/2010

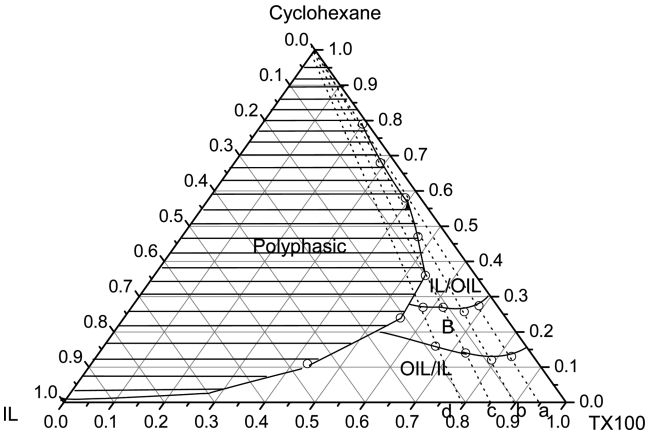

Figure 1. Phase diagram of the $[N_{3111}][Tf_2N]$/TX-100/cyclohexane three-component system at 25.0 °C. For lines a, b, c, and d, the initial TX-100 weight fractions are $I = 0.95$, 0.90, 0.85, and 0.80, respectively.

SCHEME 1: Structures of C-480 and $[N_{3111}][Tf_2N]$

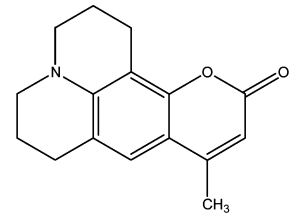

Coumarin-480

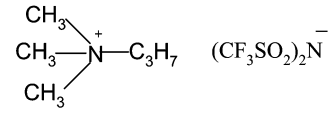

N, N, N-Trimethyl-N-propyl ammonium bis (trifluoromethanesulfonyl)imide$[N_{3111}][Tf_2N]$

been studied in the mixtures of RTILs and conventional solvents.[34b,47,48] Adhikari et al. investigated the dynamics in different regions of the 1-pentyl-3-methylimidazolium tetrafluoroborate ([pmim][BF_4]) containing microemulsions and also in neat [pmim][BF_4].[49] Mukherjee et al.[50] studied solvation of the dye, C-153, in bulk ionic liquid and in its corresponding micelle in water to address some major question regarding dynamic solvation by ionic liquids deal with whether the organic cation or the inorganic anion solvate preferentially on different time scales, the role of the correlated motion of the ion pairs and their lifetime, and the importance of translational motion of the ions relative to dipolar relaxation. Previous studies carried out by our group showed the effects of confining of the RTIL [bmim][BF_4] on solvents and rotational relaxation dynamics of C153 in TX100/cyclohexane microemulsions.[51a]

In this article, we have used nonionic surfactant TX100 as surfactant. The ternary phase diagram of the $[N_{3111}][Tf_2N]$-TX100-cyclohexane system determined at 25 °C by direct observation is illustrated in Figure 1. We also study the formation of the microemulsions using dynamic light scattering (DLS), FTIR of O−H stretching band of TX100, and also using a fluorescence probe, coumarin 480 (C480). Moreover, we investigate the solvent and rotational relaxation dynamics in this microemulsions using TCSPC with time resolution of 90 ps. The structure of RTIL and C-480 are shown in Scheme 1.

2. Experimental Section

C-480 (laser grade, Exciton) was used as received. *N*,*N*,*N*-trimethyl-*N*-propyl ammonium bis(trifluoromethanesulfonyl) imide $[N_{3111}][Tf_2N]$ was obtained from Kanto Chemicals (Japan). TX-100 was purchased from Aldrich, and cyclohexane was obtained from Spectrochem (UV spectroscopy grade). $[N_{3111}][Tf_2N]$ and TX-100 were dried in a vacuum oven for 12 h at 70−80 °C before use. A stock solution of 0.9 (M) TX100 in cyclohexane was prepared at room temperature (25 °C) by direct weighting. We used this 0.9 (M) solution for all measurements. RTIL content of the microemulsions solution (R value) was expressed by the molar ratio of added RTIL to surfactant (TX100), that is, R value = (amount of RTIL in molar unit)/(amount of TX100 in molar unit).We made the solution transparent by gentle shaking by hand. Different sizes of microemulsions were prepared by varying the molar ratio (R) of RTIL/TX-100. The final concentration of TX100 and C-480 in all experiments was kept at 0.9 and 10^{-5} (M) respectively. All experiments were carried out at 25 °C.

The absorption and fluorescence spectra were measured using a Shimadzu (model no. UV-2450) spectrophotometer and a Hitachi F-7000 fluorescence spectrophotometer. For steady-state experiments, all samples were excited at 408 nm. The time-resolved fluorescence setup is described in detail in our previous publication.[25] In brief, the samples were excited at 408 nm using a picosecond laser diode (IBH, Nanoled), and the signals were collected at the magic angle (54.7°) using a Hamamatsu microchannel plate photomultiplier tube (3809U). The instrument response function of our setup was 90 ps. The same setup was used for anisotropy measurements. For the anisotropy decays, we used a motorized polarizer in the emission side. The emission intensities at parallel ($I_{||}$) and perpendicular ($I_{\perp}$) polarizations were collected alternately until a certain peak difference between parallel ($I_{||}$) and perpendicular ($I_{\perp}$) decay was reached. The analysis of the data was done using IBH DAS (version 6) decay analysis software. The same software was also used to analyze the anisotropy data. All longer and shorter wavelength decays were fitted with biexponential and triexponential functions, respectively, because χ^2 becomes closer to 1, which indicates a good fit. For DLS measurements, we used a Malvern Nano ZS instrument employing a 4mW He−Ne laser (λ = 632.8 nm). For viscosity measurements, we used a Brookfield DV-II+ Pro (Viscometer) at 25 °C. All experiments were carried out at 298 K. The temperature was maintained as a constant (298 K) by circulating water through the cell holder using a Neslab Thermostat (RTE7). A conductivity meter manufactured by Integrated Electrolife System (India), model 213R, having an EP-type connector was used for conductance measurements. FTIR spectra of all samples were with a Perkin-Elmer FT-IR spectrometer using a ZeSe cell.

3. Results and Discussion

3.1. Phase Behavior Study. Phase behavior measurement is essential to study microemulsions. In this work, TX-100 was used as the surfactant. The ternary phase diagrams of the $[N_{3111}][Tf_2N]$/TX-100/cyclohexane system at 25 °C determined in this work by direct observation are illustrated in Figure 1. Above the phase separation boundary curve, the system exists as one phase, and the shadow area is the biphasic region. The monophasic region can be divided into different subregions, such as IL (or polar solvent)-in-oil microemulsion region (IL or polar solvent droplets dispersed in oil), oil-in-IL (or polar solvent) microemulsion region (oil droplets dispersed in IL or polar solvent), and bicontinuous region. The subareas can be conve-

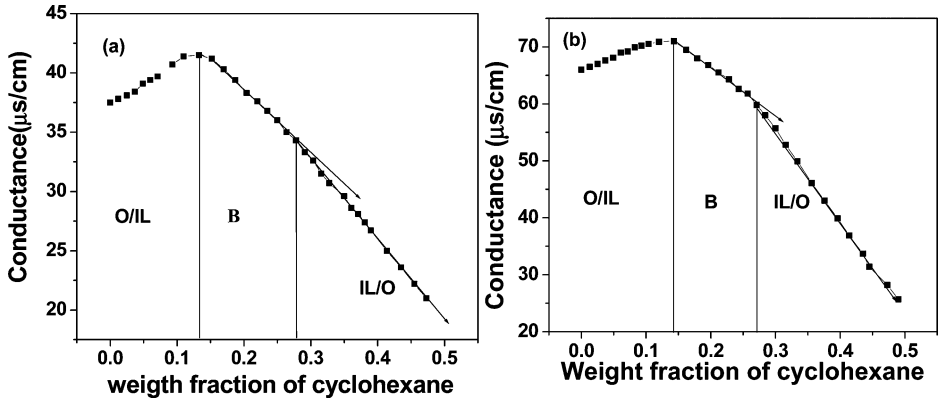

Figure 2. Electric conductivity, k, of the nonaqueous IL microemulsion as a function of cyclohexane weight content with I = (a) 0.95 and (b) 0.90, respectively.

niently located by electrical conductivity measurement.[51−53] In this work, we determined the subregions by this method. Dilution series of the microemulsions were prepared by fixing weight ratios of $[N_{3111}][Tf_2N]$/TX-100 (0.055, 0.111, 0.17, 0.22) but varying weight fraction of cyclohexane. As an example, Figure 2a,b illustrates the dependence of the conductivity on weight fraction of cyclohexane with weight ratios $[N_{3111}][Tf_2N]$/TX-100 of 0.055 and 0.111, respectively. The conductivity versus cyclohexane concentration curves were used to locate subregions using the principle and method reported by other authors,[52−54] and the subregions determined are also marked in Figure 1. In the IL/O area, the IL droplets are dispersed in the cyclohexane continuous phase, and in the O/IL region, the cyclohexane droplets are dispersed in the IL. In the bicontinuous region (marked B), there exist both IL and cyclohexane continuous phases.

3.2. IR Frequency Assignment of $[N_{3111}][Tf_2N]$/TX100/Cyclohexane Microemulsions. Infrared spectra of $[N_{3111}][Tf_2N]$/TX100/cyclohexane microemulsions containing various amounts of $[N_{3111}][Tf_2N]$ (R values) were recorded. In Figure 3a, we have shown the changes in the normalized spectra of O−H stretching bands of TX100 in the $[N_{3111}][Tf_2N]$/TX100/cyclohexane microemulsions system. With increasing $[N_{3111}][Tf_2N]$ content, the O−H stretching frequency gradually changes to lower values. For a better understanding, we have plotted the change of IR O−H stretching maxima in Figure 3b. This is possible because with increasing amount of $[N_{3111}][Tf_2N]$, the terminal hydroxyl of TX-100 is hydrogen bonded with the nitrogen atoms of the anion of $[N_{3111}][Tf_2N]$, which results in the OH stretching band appearing in the low-frequency region of the IR spectrum. This interaction might be the driving force for solubilizing of $[N_{3111}][Tf_2N]$ into the core of the TX-100 aggregates.

3.3. Dynamic Light Scattering and Formation of $[N_{3111}][Tf_2N]$/TX-100/Cyclohexane Microemulsions. DLS of a mixture of TX-100 and $[N_{3111}][Tf_2N]$ in cyclohexane indicates the formation of microemulsions. The results are shown in Figure 4. At a $[N_{3111}][Tf_2N]$/TX-100 molar ratio, $R = 0.30$, the average hydrodynamic diameter is found to be 23 nm. The larger droplet (microemulsions) size for the $[N_{3111}][Tf_2N]$/TX-100/cyclohexane system suggests the formation of a polar domain ("pool") containing the RTIL.

3.4. Viscosity Measurement. We have measured the viscosity of neat $[N_{3111}][Tf_2N]$- and $[N_{3111}][Tf_2N]$-containing microemulsions at 25 °C. With gradual addition of $[N_{3111}][Tf_2N]$ to the TX-100/cyclohexane solution, the bulk viscosity of the solution gradually increases. The bulk viscosities of $[N_{3111}][Tf_2N]$- and $[N_{3111}][Tf_2N]$-containing microemulsions at 25 °C are listed in (Table 4).

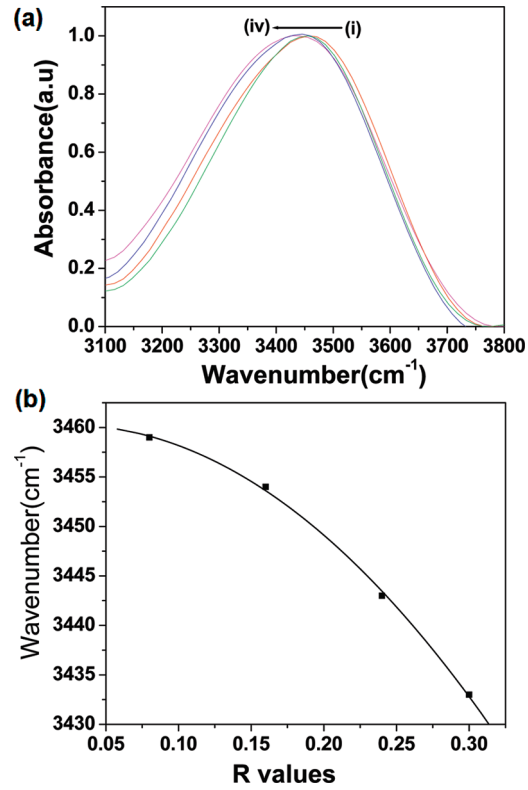

Figure 3. (a) Change of O−H stretching band of TX100 in the $N_{3111}Tf_2N$/TX100/cyclohexane microemulsions system at different R values: R = (i) 0.08, (ii) 0.16, (iii) 0.24, and (iv) 0.30, respectively. (b) Variation of O−H stretching frequency of TX100 in the $N_{3111}Tf_2N$/TX100/cyclohexane microemulsions system.

3.5. Steady-State Absorption and Emission Spectra. The absorption and emission spectra were taken in cyclohexane and in $[N_{3111}][Tf_2N]$ microemulsions. The absorption and emission maxima are listed in Table 1. The emission maxima of C-480 in cyclohexane and $[N_{3111}][Tf_2N]$ ionic liquid are 410 and 461 nm, respectively. On addition of TX-100 to a solution of C-480 in cyclohexane, the emission maximum of C-480 exhibits a marked red shift from 410 to 451 nm. The marked red shift by 41 nm indicates transfer of the C-480 molecules from bulk cyclohexane to the interior of TX-100 reverse micelle. On addition of the RTIL $[N_{3111}][Tf_2N]$ to the TX-100/cyclohexane mixture, the emission maximum of C-480 displays a further red shift by 8 to 459 nm (at $\lambda_{ex} = 410$ nm, Figure 5b). The red shift suggests that the probe C-480 is located inside the polar

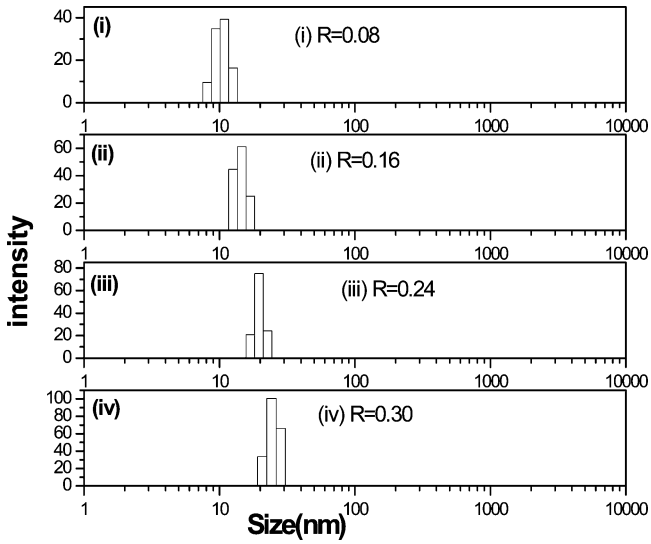

Figure 4. Size distribution of the droplets (measured by dynamic light scattring) in a microemulsions of $[N_{3111}][Tf_2N]$/TX-100/cyclohexane for R = (i) 0.08,(ii) 0.16, (iii) 0.24, and (iv) 0.30.

TABLE 1: Steady-State Absorption and Emission Maxima of C-480 in Neat $[N_{3111}][Tf_2N]$ and in $[N_{3111}][Tf_2N]$/TX100/ Cyclohexane Microemulsions

systems	absorption maxima (nm)	emission maxima (nm)
TX100/cyclohexane (R = 0.00) + C-480	378	452
$[N_{3111}][Tf_2N]$/TX100/cyclohexane/ (R = 0.08) + C-480	379	455
$[N_{3111}][Tf_2N]$/TX100/cyclohexane/ (R = 0.16) + C-480	380	457
$[N_{3111}][Tf_2N]$/TX100/cyclohexane/ (R = 0.24) + C-480	381	458
$[N_{3111}][Tf_2N]$/TX100/cyclohexane/ (R = 0.30) + C-480	381	459
Neat $[N_{3111}][Tf_2N]$ + C-480	384	461

domain ("pool" of the RTIL). It is important to note that the emission maximum of C-480 in the microemulsions (459 nm) is different from that in neat $[N_{3111}][Tf_2N]$ (461 nm). The absorbance at the red end side increases with the addition of $[N_{3111}][Tf_2N]$ to the C-480/cyclohexane/TX-100 solution. This indicates that a substantial number of C-480 molecules migrate from bulk solvent to the core of ionic liquid pool of microemulsions. The absorption and emissions spectra of C-480 are illustrated in Figure 5a,b, respectively.

3.6. Time-Resolved Studies. ***3.6.1. Time-Resolved Anisotropy Measurements.*** Absorption and emission spectra can give a qualitative idea regarding the location of the probe molecules. This can be more accurately predicted by the time-resolved fluorescence anisotropy. Time resolved anisotropy, $r(t)$, is calculated using the following equation

$$r(t) = \frac{I_{\parallel}(t) - GI_{\perp}(t)}{I_{\parallel}(t) + 2GI_{\perp}(t)} \quad (1)$$

where G is the correction factor for detector sensitivity to the polarization direction of emission. $I_{\parallel}(t)$ and $I_{\perp}(t)$ are fluorescence decays polarized parallel and perpendicular to the polarization of the excitation light respectively. The G factor for our setup is 0.6. The anisotropy decay parameters are listed in Table 3. Representative anisotropy decays of C-480 in microemulsions

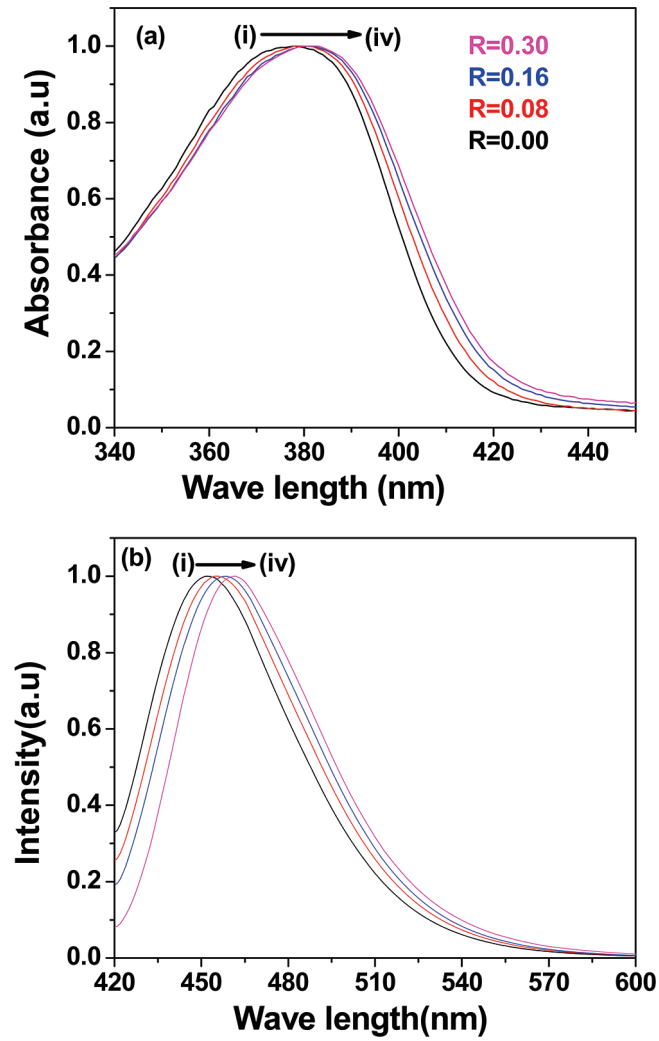

Figure 5. (a) Absorption spectrum of C-480 in (i) TX100-cyclohexane mixture (1.1:0.7 ratio) and $[N_{3111}][Tf_2N]$/TX100/cyclohexane microemulsions R = (ii) 0.08, (iii) 0.16, and (iv) 0.30, respectively. (b) Emission spectrum of C-480 in (i) TX100-cyclohexane mixture (1.1:0.7 ratio) and $[N_{3111}][Tf_2N]$/TX100/cyclohexane microemulsions R = (ii) 0.08 and (iii) 0.30 and (iv) in neat $[N_{3111}][Tf_2N]$, respectively.

at R = 0, 0.08, and 0.30 are shown in Figure 6. The anisotropy decays in microemulsions are found to be triexponential in nature. We previously reported that C-480 has a rotational time of ~80 ps in pure cyclohexane.[51b] Table 3 reveals that rotational relaxation times of C-480 are much longer in microemulsions compared with that in cyclohexane. Moreover, the anisotropy decays of the probe molecules in the presence and absence of $[N_{3111}][Tf_2N]$ are different. The rotational relaxation times of C-480 at R = 0, that is, without addition of $[N_{3111}][Tf_2N]$, is 0.82 ns. With the addition of $[N_{3111}][Tf_2N]$, the rotational time increases, and at R = 0.08, 0.16, 0.24, and 0.30, the rotational relaxation times for C-480 become 1.30, 1.37, 1.85, and 1.91 ns, respectively. The high rotational relaxation times in the presence of $[N_{3111}][Tf_2N]$ indicate that the probe molecules experience a different environment inside the $[N_{3111}][Tf_2N]$ pool from that in pure cyclohexane or TX100-cyclohexane mixture.

In bulk cyclohexane, the time constant of fluorescence anisotropy decay of C-480 is 80 ps. In neat ($[N_{3111}][Tf_2N]$), C-480 exhibits a very slow rotational dynamics with a single exponential decay of time constant, 3.35 ns. The anisotropy decay of C-480 in TX-100/cyclohexane is found to be quite fast with a time constant of 0.82 ns. On addition of the ionic

TABLE 2: Decay Parameters of Solvent Correlation Function $C(t)$ of C-480 in $[N_{3111}][Tf_2N]$/TX100/Cyclohexane Microemulsions

systems	α_1	α_2	α_3	τ_1 (ns)	τ_2 (ns)	τ_3 (ns)	$\langle\tau\rangle_{av}$ (ns)
$[N_{3111}][Tf_2N]$/TX100/ cyclohexane $R = 0.08$ C-480	0.29	0.44	0.27	0.04	0.96	14.00	4.21
$[N_{3111}][Tf_2N]$/TX100/ cyclohexane $R = 0.30$ C-480	0.35	0.41	0.24	0.04	0.93	10.26	2.86
neat $[N_{3111}][Tf_2N]$ + C-480	0.67	0.33		0.04	0.56		0.21

TABLE 3: O−H Stretching Frequency of TX100 and Size of the $[N_{3111}][Tf_2N]$/TX100/Cyclohexane Microemulsions System

systems	O−H stretching frequency (cm^{-1})	size (nm)
TX100/$[N_{3111}][Tf_2N]$/ cyclohexane $R = 0.08$ C-480	3459	10
TX100/$[N_{3111}][Tf_2N]$/ cyclohexane $R = 0.16$ C-480	3454	13
TX100/$[N_{3111}][Tf_2N]$/ cyclohexane $R = 0.24$ C-480	3443	18
TX100/$[N_{3111}][Tf_2N]$/ cyclohexane $R = 0.30$ C-480	3433	23

liquid $[N_{3111}][Tf_2N]$ to the TX-100/cyclohexane reverse micelle, the anisotropy decay of C-480 slows down markedly with the emergence of two additional components (Figure 6 and Table 4). This suggests that within the $[N_{3111}][Tf_2N]$ containing microemulsions, C-480 probes are distributed in three broadly different regions: a very fast region near the bulk cyclohexane of rotational relaxation time around 100 ps, a fast region near headgroup of TX-100 of rotational relaxation time 0.82 ns, and a slow region of rotational relaxation time 2 to 3 ns at the pool of the RTIL. The average rotational time is found to be 0.82, 1.30, and 1.91 ns for $R = 0$, 0.08, and 0.30, respectively (R = [RTIL]/[TX-100]). This is due to the fact that with the addition of more and more RTIL, the viscosity of the RTIL pool increases; hence we see an increase in the average rotational relaxation time. It is interesting to note that with increasing RTIL in microemulsions, the magnitude of the slow components increases; consequently, average rotational relaxation time increases. C-480 exhibits a very slow rotational dynamics

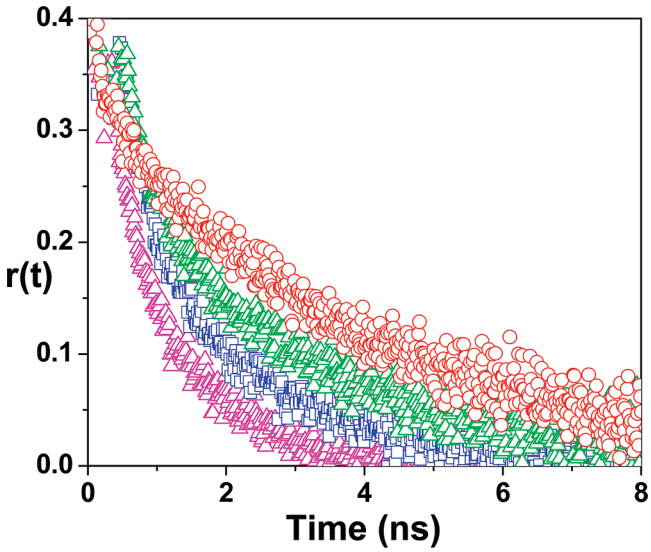

Figure 6. Fluorescence anisotropy decay of C-480 in (i) neat $[N_{3111}][Tf_2N]$ (○) and (ii) TX100-cyclohexane mixture (1.1:0.7 weight ratio) $[N_{3111}][Tf_2N]$/TX100/cyclohexane microemulsions (△) at (iii) $R = 0.08$ (□) and (iv) $R = 0.30$ (△), respectively.

(Figure 6) with a single exponential decay of time constant of 3.37 ns in neat RTIL. The slow anisotropy decay in neat ionic liquid may obviously be ascribed to the high viscosity of $[N_{3111}][Tf_2N]$. The interesting observation is that the rotational relaxation times in the RTIL containing microemulsions are faster than that in neat $[N_{3111}][Tf_2N]$. This is due to broad distribution of probe molecules in three different regions of microemulsions.

3.6.2. Solvation Dynamics. To study solvent relaxation dynamics, we collected the time-resolved decays monitored at different wavelength for all the systems. The decays at the red edge of the emission spectra were preceded by a growth in fraction of nanosecond time scale, whereas decays at the short wavelengths are fast. The wavelength-dependent behavior of temporal decays of C-480 clearly indicates that solvent relaxation is taking place in these systems. The representative decays of C-480 monitoring at three different wavelengths are shown in Figure 1 of the Supporting Information. The TRES were constructed using the procedure of Fleming and Maroncelli.[55] The TRES at a given time t, $S(\lambda,t)$, is obtained by the fitted decays, $D(t,\lambda)$, by relative normalization to the steady-state spectrum $S_0(\lambda)$, as follows

$$S(\lambda, t) = D(\lambda, t)\frac{S_0(\lambda)}{\int_0^\infty D(\lambda, t)\,\mathrm{d}t} \tag{2}$$

Each TRES was fitted by a log-normal line shape function, which is defined as

$$g(\nu) = g_0 \exp\left[-\ln 2\left(\frac{\ln[1 + 2b(\nu - \nu_p)]/\Delta}{b}\right)^2\right] \tag{3}$$

where g_0, b, ν_p, and Δ are the peak height, asymmetric parameter, peak frequency, and width parameter, respectively. A representative TRES of C-480 in $[N_{3111}][Tf_2N]$/TX100/cyclohexane ($R = 0.08$) microemulsions at 298 K is shown in Figure 2 of the Supporting Information. We have obtained the peak frequency from the log-normal fitting of TRES. The solvation dynamics was monitored by the solvent response function defined as

$$C(t) = \frac{\nu(t) - \nu(\infty)}{\nu(t = 0) - \nu(\infty)} \tag{4}$$

$\nu(t = 0)$ is the frequency at "zero-time", as calculated by the method of Fleming and Maroncelli.[55] $\nu(\text{“}\infty\text{”})$ is the frequency at "infinite time", which may be taken as the maximum of the steady-state fluorescence spectrum if solvation is more rapid than the population decay of the probe. $\nu(t)$ is determined by taking the maxima from the log-normal fits as the emission maximum. In most of the cases, however, the spectra are broad, so there is some uncertainty in the exact position of the emission

TABLE 4: Decay Parameters of Rotational Relaxation of C-480 in $[N_{3111}][Tf_2N]$/TX100/Cyclohexane Microemulsions

systems	α_1	α_2	α_3	τ_1 (ns)	τ_2 (ns)	τ_3 (ns)	$\langle\tau\rangle_{av}$ (ns)	R_0	viscosity (cP)
TX100/cyclohexane/C-480	1			0.82			0.82	0.29	20
TX100/$[N_{3111}][Tf_2N]$/ cyclohexane $R = 0.08$ C-480	0.35	0.57	0.08	0.45	2.00	0.07	1.30	0.37	25
TX100/$[N_{3111}][Tf_2N]$/ cyclohexane $R = 0.16$ C-480	0.31	0.49	0.20	0.63	2.36	0.11	1.37	0.39	29
TX100/$[N_{3111}][Tf_2N]$/ cyclohexane $R = 0.24$ C-480	0.34	0.50	0.16	0.69	3.20	0.09	1.85	0.38	34
TX100/$[N_{3111}][Tf_2N]$/ cyclohexane $R = 0.30$ C-480	0.33	0.54	0.13	0.64	3.12	0.08	1.91	0.39	38
$[N_{3111}][Tf_2N]$ + C-480		1.00			3.35		3.35	0.31	74

maxima. Therefore, we have considered the range of the raw data points in the neighborhood of the maximum to estimate an error for the maximum obtained from the log-normal fit. Depending on the width of the spectrum (i.e., zero-time, steady-state, or TRES), we have determined the typical uncertainties as follows: zero time ≈ steady-state (± 120 cm^{-1}) < time-resolved (± 200 cm^{-1}) emission. We use these uncertainties to compute error bars for $C(t)$. Finally, in generating $C(t)$, the first point was obtained from the zero time spectrum. The second point was taken at the maximum of the instrument response function, which, having a full width at half-maximum of ≤100 ps, was taken to be 100 ps. The solvent response function ($C(t)$) was fitted to a triexponential decay function

$$C(t) = a_1 \exp^{(-t/\tau_1)} + a_2 \exp^{(-t/\tau_2)} + a_3 \exp^{(-t/\tau_3)} \quad (5)$$

where τ_1, τ_2, and τ_3 are the relaxation times with amplitude α_1, a_2, and α_3, respectively.

At first, we are going to discuss the important features of solvation dynamics in pure RTILs. It should be noted that solvation dynamics in RTILs are vastly different from that in the isopolar conventional solvents such as methanol, acetonitrile, and so on.[56,57] Solvation in RTILs takes place because of the motion of the ions around an excited dye, whereas in water, methanol, and acetonitrile, that is, in polar solvents, solvation takes place as the solvent molecules reorient themselves around an excited dye. Recent ultrafast studies suggest that the difference is less striking than originally thought.[33,44a] Chapman and Maroncelli[58] showed that ionic solvation is slower compared with the pure solvent and dependent on the viscosity of the medium. Samanta and coworkers observed biphasic solvation dynamics in different RTILs.[42] They ascribed the fast component to the motion of the anions, and the slow component is ascribed to the collective motions of the both cation and anions, respectively. Petrich and coworkers observed that the polarizability of the cation is responsible for the fast component.[59] Song observed the similar phenomenon regarding fast components using Debye−Huckel dielectric continuum model. Halder et al.[60,61] suggest that translational motion of ions may not be the predominant factor in the short time solvation of ionic fluids. According to Maroncelli et al.[44c−e] the fast component arises because of the translation adjustment of the ions within the solvation structure present at the time of solute excitation. Kobrak et al.[62] also showed that collective cation−anion motions are responsible for the fast component. Shim et al.[63] suggested that ultrafast dynamics is dependent on the local density of the ions near the probe molecules.

To comprehend the solvation dynamics results, a thorough understanding of the microemulsions structure and location of the probe within the microemulsions is necessary. UV, fluorescence, and anisotropy study showed that a substantial number of probe molecule reside in the core of the microemulsions. DLS experiments show that the structure of the microemulsions is spherical and that the hydrodynamic diameter increases from 10 to 23 nm as R varies from 0.08 to 0.30. On addition of the ionic liquid $[N_{3111}][Tf_2N]$ to the TX100/cyclohexane reverse micelle, the solvent relaxation of C-480 is faster (Figure 7 and Table 2). At different R values of the $[N_{3111}][Tf_2N]$ microemulsions, we have observed slow bimodal solvation dynamics. We observed 4.21 ns average solvation time in $[N_{3111}][Tf_2N]$/TX100/cyclohexane microemulsions when the molar ratio (R) of RTIL

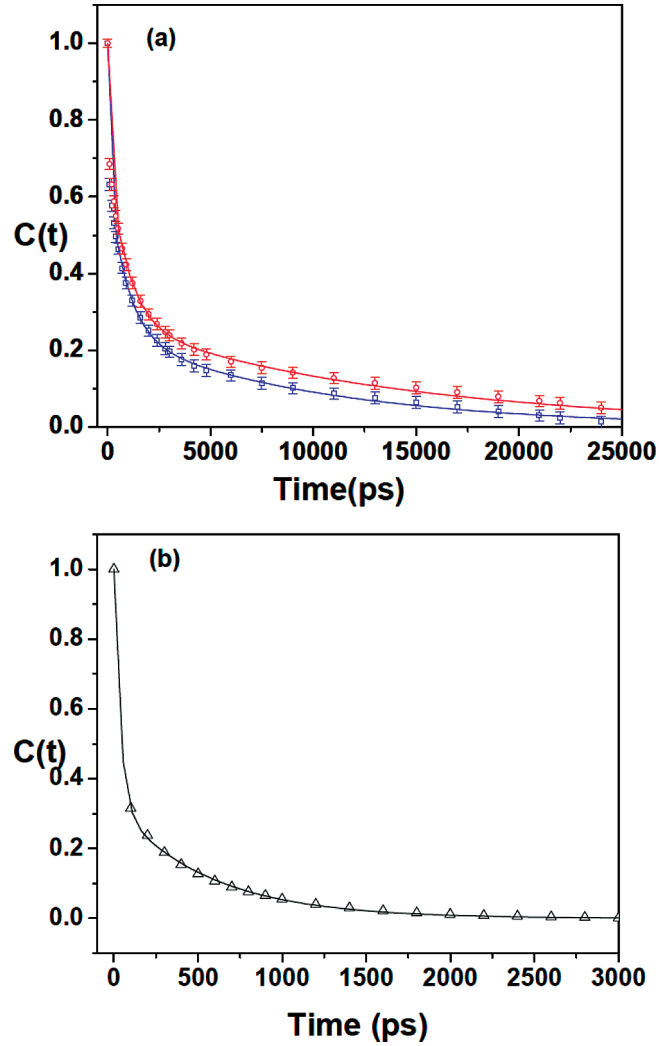

Figure 7. (a) Decay of solvent correlation function of $C(t)$ in $[N_{3111}][Tf_2N]$/TX100/cyclohexane microemulsions at R = (i) 0.08 (○) and (iii) 0.30 (□), respectively. (b) Decay of solvent correlation function of $C(t)$ in neat $[N_{3111}][Tf_2N]$.

and TX100 is 0.08. The value of the fast component was 0.96 ns, and that of the slow component was 14.0 ns with relative contribution of 44 and 27%, respectively. In the microemulsion at $R = 0.30$, that is, with higher RTIL content, we observed 2.86 ns average solvation time, and the value of the fast component was 0.93 ns and that of the slow component was 10.26 ns with relative contribution 41 and 24%, respectively. We also observed a very fast components with time constant around 40 ps, and the relative contributions of the component are 29 and 35% at $R = 0.08$ and 0.30, respectively. We have also measured solvent relaxation in neat $[N_{3111}][Tf_2N]$ and the average solvation time of C-480 is 0.21 ns with components 0.04 (67%) and 0.56 ns (33%).

From $C(t)$ parameters, we got ultrafast components with time constants around 40 ps in neat RTIL as well as RTIL containing microemulsions at different R values. The magnitude of the components is beyond that of the instrument resolution (90 ps). We have fitted the time zero spectrum using the Fee and Maroncelli method, and thus we can obtain the ultrafast components. The ultrafast components are actually the missing dynamics in the studied systems. There may be more than one ultrafast components present in these systems, and the average of these ultrafast components is ~40 ps, which we are missing in our time-resolved setup.

The fast components remain almost unchanged, whereas the slower components became faster. We also observed the relative contribution of the faster component, and the slower components decrease at higher R values. Although the values of faster components are unchanged, the relative contribution of the faster and the slower components decreases, and the slower components became faster so we observed a decrease in average solvation time. For example, when we use 0.30 molar ratios (R) RTIL, we got faster component 0.93 ns having relative contribution of 41% and slower component 10.26 ns having relative contribution of 24%. Therefore, the average solvation time varies from 4.21 to 2.86 ns as R is increasing from 0.08 to 0.30. (See Table 2.) The increase in $[N_{3111}][Tf_2N]$ contents (because of the increase in the R values) increases the size of the microemulsions. The decrease in solvation time with an increase in the in R value is due to the increase in the sizes of the microemulsions. Because in RTIL solvation depends on the motions of ions, if motions of ions are slow, then solvation is slower, and if motions of ions are fast, then solvation are faster. The increase in size leads to the increase in the free motion of the ions in the core of microemulsions, which, consequently, decreases the solvation time.

4. Conclusions

In summary, microemulsions consisting of $[N_{3111}][Tf_2N]$, surfactant TX-100, and cyclohexane were prepared, and the phase behavior of the ternary system was investigated. The $[N_{3111}][Tf_2N]$-in-cyclohexane (IL/O), bicontinuous, and cyclohexane-in-$[N_{3111}][Tf_2N]$ (O/IL) microregions of the nonaqueous RTIL microemulsions were initially identified by traditional electrical conductivity measurements on the basis of percolation theory. FTIR data of O−H stretching band of TX100 support the formation of $[N_{3111}][Tf_2N]$/TX100/cyclohexane microemulsions. Steady-state and time-resolved fluorescence spectroscopy have been used to investigate the structure and dynamical behavior of $[N_{3111}][Tf_2N]$/TX100/cyclohexane microemulsions with variation of ionic liquid content. The motions of the ions of RTILs are responsible for the slow solvation. Because the size of the microemulsions increases with gradual addition of $[N_{3111}][Tf_2N]$, movements of ions of RTILs are less restricted in the cores of the microemulsions with consequently faster solvation dynamics of RTILs in the microemulsions core with increasing amount of $[N_{3111}][Tf_2N]$. With the addition of more and more ionic liquid in microemulsions, the microviscosity of the ionic liquid pools increases consequently rotational relaxation time of C-480 increases.

Acknowledgment. N.S. is thankful to Department of Science and Technology (DST) and BRNS, (Govt. of India) for generous research grants. R.P., C.G., and V.G.R. are thankful to CSIR for research fellowships. S.S. is thankful to BRNS for SRF.

Supporting Information Available: Time-resolved decays and spectra. This material is available free of charge via the Internet at http://pubs.acs.org.

References and Notes

(1) (a) Seddon, K. R. *Nature* **2003**, *2*, 363. (b) Welton, T. *Chem. Rev* **1999**, *99*, 2071.
(2) (a) Zhao, D.; Wu, M.; Kou, Y.; Min, E. *Catal. Today* **2002**, *74*, 157. (b) Parvulescu, V. I.; Hardacre, C. *Chem. Rev.* **2007**, *107*, 2615. (c) Haumann, M.; Riisager, A. *Chem. Rev.* **2008**, *108*, 1474. (d) Plechkova, N. V.; Seddon, K. R. *Chem. Soc. Rev.* **2008**, *37*, 123. (e) Rantwijk, F.; van; Sheldon, R. A. *Chem. Rev.* **2007**, *107*, 2757.
(3) Solans, C.; Kunieda, H. *Industrial Applications of Microemulsions*; Surfactant Science Series; Dekker: New York, 1997; Vol. 66.
(4) Johnston, K. P.; Harrison, K. L.; Clarke, M. J.; Howdle, S. M.; Heitz, M. P.; Bright, F. V.; Carlier, C.; Randolph, T. W. *Science* **1996**, *271*, 624.
(5) Beckman, E. J. *Science* **1996**, *271*, 613.
(6) Challa, V.; Kuta, K.; Lopina, S.; Cheung, H. M.; Meerwall, E. V. *Langmuir* **2003**, *19*, 4154.
(7) Hermanson, K. D.; Kaler, E. W. *Macromolecules* **2003**, *36*, 1836.
(8) Li, M.; Schnablegger, H.; Mann, S. *Nature* **1999**, *402*, 393.
(9) Venables, D. S.; Huang, K.; Schmuttenmaer, C. A. *J. Phys. Chem. B* **2001**, *105*, 9132.
(10) (a) Willard, D. M.; Riter, R. E.; Levinger, N. E. *J. Am. Chem. Soc.* **1998**, *120*, 4151. (b) Riter, R. E.; Undiks, E. P.; Levinger, N. E. *J. Am. Chem. Soc.* **1998**, *120*, 6062.
(11) Nandi, N.; Bhattacharyya, K.; Bagchi, B. *Chem. Rev.* **2000**, *100*, 2013.
(12) Boyd, J. E.; Briskman, A.; Sayes, C.; Mittleman, M.; Colvin, D. V. *J. Phys. Chem. B* **2002**, *106*, 6346.
(13) Wasserscheid, P.; Welton, T. *Ionic Liquids in Synthesis*; Wiley-VCH: Weinheim, Germany, 2002.
(14) Dupont, J.; de Souza, R. F.; Suarez, P. A. Z. *Chem. Rev.* **2002**, *102*, 3667.
(15) Cole, A. C.; Jensen, J. L.; Ntai, I.; Tran, K. L. T.; Weaver, K. J.; Forbes, Jr., D. C.; Davis, J. H. *J. Am. Chem. Soc.* **2002**, *124*, 5962.
(16) Brown, R. A.; Pollet, P.; McKoon, E.; Eckert, C. A.; Liotta, C. L.; Jessop, P. G. *J. Am. Chem. Soc.* **2001**, *123*, 1254.
(17) Blanchard, L. A.; Hancu, D.; Beckman, E. J.; Brennecke, J. F. *Nature* **1999**, *399*, 28.
(18) Kahlweit, M.; Strey, R. *Angew. Chem., Int. Ed. Engl.* **1985**, *24*, 654.
(19) Kahlweit, M.; Strey, R.; Firman, P.; Haase, D.; Jen, J.; Schomacker, R. *Langmuir* **1988**, *4*, 499.
(20) Kahlweit, M.; Strey, R.; Firman, P. *J. Phys. Chem.* **1986**, *90*, 671.
(21) Kahlweit, M.; Strey, R.; Busse, G. *J. Phys. Chem.* **1990**, *94*, 3881.
(22) Sottmann, T.; Strey, R. In *Soft Colloids V: Fundamentals in Interface and Colloid Science*; Lyklema, J., Ed.; Elsevier: Amsterdam, 2005; Ch. 5.
(23) Gao, H. X.; Li, J. C.; Han, B. X.; Chen, W. N.; Zhang, J. L.; Zhang, R. *Phys. Chem. Chem. Phys.* **2004**, 2914.
(24) Fletcher, K. A.; Pandey, S. *Langmuir* **2004**, *20*, 33.
(25) Cheng, S.; Zhnag, J.; Zhang, Z.; Han, B. *Chem. Commun.* **2007**, 2497.
(26) Gao, Y.; Han, S.; Han, B.; Li, G.; Shen, D.; Li, Z.; Du, J.; Hou, W.; Zhang, G. *Langmuir* **2005**, *21*, 5681.
(27) Eastoe, J.; Gold, S.; Rogers, S. E.; Paul, A.; Welton, T.; Heenan, R. K.; Grillo, I. *J. Am. Chem. Soc.* **2005**, *127*, 7302.
(28) Patrascu, C.; Gauffre, F.; Nallet, F.; Bordes, R.; Oberdisse, J.; de Lauth- Viguerie, N.; Mingotaud, C. *Chem. Phys. Chem.* **2006**, *7*, 99.
(29) (a) Takahashi, K.; Sakai, S.; Tezuka, H.; Heijima, Y.; Katsumura, Y.; Watanabe, M. *J. Phys. Chem. B* **2007**, *111*, 4807. (b) Shim, Y.; Jeong, D.; Manjari, S.; Choi, M. D.; Kim, H. J. *Acc. Chem. Res.* **2007**, *40*, 1130.
(30) Reichardt, C. *Green Chem.* **2005**, *7*, 339.
(31) Reichardt, C. *Org. Process Res. Dev.* **2007**, *11*, 105.

(32) (a) Paul, A.; Samanta, A. *J. Phys. Chem. B* **2007**, *111*, 4724. (b) Karmakar, R.; Samanta, A. *J. Phys. Chem. A* **2003**, *107*, 7340.

(33) Arzhantsev, S.; Jin, H.; Baker, G. A.; Maroncelli, M. *J. Phys. Chem. B.* **2007**, *111*, 4978.

(34) (a) Lang, B.; Angulo, G.; Vauthey, E. *J. Phys. Chem. A* **2006**, *110*, 7028. (b) Baker, S. N.; Baker, G. A.; Munson, C. A.; Chen, F.; Bukowski, E. J.; Cartwright, A. N.; Bright, F. V. *Ind. Eng. Chem. Res.* **2003**, *42*, 6457.

(35) Hu, Z.; Margulis, C. J. *Acc. Chem. Res.* **2007**, *40*, 1097.

(36) Adhikari, A.; Dey, S.; Das, D. K.; Mandal, U.; Ghosh, S.; Bhattacharyya, K. *J. Phys. Chem. B* **2008**, *112*, 6350.

(37) (a) Shirota, H.; Castner, E. W., Jr. *J. Phys. Chem. B* **2005**, *109*, 21576. (b) Shirota, H.; Wishart, J. F.; Castner, E. W., Jr. *J. Phys. Chem. B* **2007**, *111*, 4819.

(38) Chung, S. H.; Lopato, R.; Greenbaum, S. G.; Shirota, H.; Castner, E. W., Jr,; Wishart, J. F. *J. Phys. Chem. B* **2007**, *111*, 4885.

(39) (a) Chakrabarty, D.; Chakraborty, A.; Hazra, P.; Seth, D.; Sarkar, N. *Chem. Phys. Lett.* **2004**, *397*, 216. (b) Karmakar, R.; Samanta, A. *Chem. Phys. Lett.* **2003**, *376*, 638.

(40) Ito, N.; Arzhantsev, S.; Maroncelli, M. *Chem. Phys. Lett.* **2004**, *396*, 83.

(41) (a) Chakrabarty, D.; Hazra, P.; Chakraborty, A.; Seth, D.; Sarkar, N. *Chem. Phys. Lett.* **2003**, *381*, 697. (b) Seth, D.; Sarkar, S.; Sarkar, N. *J. Phys. Chem. B* **2008**, *112*, 2629.

(42) (a) Karmakar, R.; Samanta, A. *J. Phys. Chem. A* **2002**, *106*, 4447. (b) Karmakar, R.; Samanta, A. *J. Phys. Chem. A* **2002**, *106*, 6670. (c) Karmakar, R.; Samanta, A. *J. Phys. Chem. A* **2003**, *107*, 7340.

(43) (a) Samanta, A. *J. Phys. Chem. B* **2006**, *110*, 13704. (b) Paul, A.; Mandal, P. K.; Samanta, A. *J. Phys. Chem. B* **2005**, *109*, 9148. (c) Aki, S. N. V. K.; Brennecke, J. F.; Samanta, A. *Chem. Commun.* **2001**, 413. (d) Mandal, P. K.; Paul, A.; Samanta, A. *J. Photochem. Photobiol., A* **2006**, *182*, 113.

(44) (a) Jin, H.; Baker, G. A.; Arzhantsev, S.; Dong, J.; Maroncelli, M. *J. Phys. Chem. B* **2007**, *111*, 7291. (b) Ito, N.; Arzhantsev, S.; Heitz, M.; Maroncelli, M. *J. Phys. Chem. B* **2004**, *108*, 5771. (c) Ingram, J. A.; Moog, R. S.; Ito, N.; Biswas, R.; Maroncelli, M. *J. Phys. Chem. B* **2003**, *107*, 5926. (d) Arzhantsev, S.; Ito, N.; Heitz, M.; Maroncelli, M. *Chem. Phys. Lett.* **2003**, *381*, 278. (e) Ito, N.; Arzhantsev, S.; Maroncelli, M. *Chem. Phys. Lett.* **2004**, *396*, 83.

(45) (a) Funston, A. M.; Fadeeva, T. A.; Wishart, J. F.; Castner, E. W., Jr. *J. Phys. Chem. B* **2007**, *111*, 4963. (b) Shirota, H.; Castner, E. W., Jr. *J. Phys. Chem. A* **2005**, *109*, 9388.

(46) (a) Kobrak, M. N. *J. Chem. Phys.* **2006**, *125*, 064502. (b) Jeong, D.; Shim, Y.; Choi, M. Y.; Kim, H. J. *J. Phys. Chem. B* **2007**, *111*, 4920. (c) Bhargava, B. L.; Balasubramanian, S. *J. Chem. Phys.* **2006**, *125*, 219901. (d) Huang, X. H.; Margulis, C. J.; Li, Y. H.; Berne, B. J. *J. Am. Chem. Soc.* **2005**, *127*, 17842. (e) Liu, X.; Zhou, G.; Zhang, S.; Wu, G.; Yu, G. *J. Phys. Chem. B* **2007**, *111*, 5658. (f) Ghatee, M. H.; Ansari, Y. *J. Chem. Phys.* **2007**, *126*, 154502. (g) Kashyap, H. K.; Biswas, R. *J. Phys. Chem. B.* **2008**, *112*, 12431.

(47) Chakrabarty, D.; Chakraborty, A.; Seth, D.; Sarkar, N. *J. Phys. Chem. A* **2005**, *109*, 1764.

(48) Paul, A.; Samanta, A. *J. Phys. Chem. B* **2008**, *112*, 947.

(49) Adhikari, A.; Sahu, K.; Dey, S.; Ghosh, S.; Mandal, U.; Bhattacharyya, K. *J. Phys. Chem. B* **2007**, *111*, 12809.

(50) (a) Mukherjee, P.; Crank, J. A.; Halder, M.; Armstrong, D. W.; Petrich, J. W. *J. Phys. Chem. A* **2006**, *110*, 10725. (b) Mukherjee, P.; Crank, J. A.; Sharma, P. S.; Wijeratne, A. B.; Adhikary, R.; Bose, S.; Armstrong, D. W.; Petrich, J. W. *J. Phys. Chem. B* **2008**, *112*, 3390.

(51) (a) Chakrabarty, D.; Seth, D.; Chakraborty, A.; Sarkar, N. *J. Phys. Chem. B* **2005**, *109*, 5753. (b) Hazra, P.; Chakrabarty, D.; Chakraborty, A.; Sarkar, N. *Chem. Phys. Lett.* **2003**, *382*, 71.

(52) Clausse, M.; Peyrelasse, J.; Hell, J.; Boned, C.; Lagourette, B. *Nature* **1981**, *293*, 636.

(53) Raj, W. R. P.; Sasthav, M.; Cheung, M. H. *Langmuir* **1991**, *7*, 2586.

(54) Kirkpartrick, S. *Phys. Rev. Lett.* **1971**, *27*, 1722.

(55) Maroncelli, M.; Fleming, G. R. *J. Chem. Phys.* **1987**, *86*, 6221.

(56) (a) Vajda, S.; Jimenez, R.; Rosenthal, S. J.; Fidler, V.; Fleming, G. R.; Castner, E. W., Jr. *J. Chem. Soc., Faraday Trans.* **1994**, *91*, 867. (b) Kahlow, M. A.; Kang, T. J.; Barbara, P. F. *J. Chem. Phys.* **1988**, *88*, 2372.

(57) (a) Maroncelli, M. *J. Mol. Liq.* **1993**, *57*, 1. (b) Horng, M. L.; Gardecki, J. A.; Papazyan, A.; Maroncelli, M. *J. Phys. Chem.* **1995**, *99*, 17311.

(58) Chapman, C. F.; Maroncelli, M. *J. Phys. Chem.* **1991**, *95*, 9095.

(59) Headley, L. S.; Mukherjee, P.; Anderson, J. L.; Ding, R.; Halder, M.; Armstrong, D. W.; Song, X.; Petrich, J. W. *J. Phys. Chem. A* **2006**, *110*, 9549.

(60) Song, X. *J. Chem. Phys.* **2009**, *131*, 044503.

(61) Halder, M.; Headley, L. S.; Mukherjee, P.; Song, X.; Petrich, J. W. *J. Phys. Chem. A* **2006**, *110*, 8623.

(62) Kobrak, M. N.; Znamenskiy, V. *Chem. Phys. Lett.* **2004**, *395*, 127.

(63) (a) Shim, Y.; Duan, J. S.; Choi, M. Y.; Kim, H. J. *J. Chem. Phys.* **2003**, *119*, 6411. (b) Shim, Y.; Choi, M. Y.; Kim, H. J. *J. Chem. Phys.* **2005**, *122*, 044511.

JP1017086